CHAPTER THREE

HEAT AND MASS TRANSFER AND TWO-PHASE FLOW I

Jen-Shih Chang
Department of Engineering Physics &
Institute for Energy Studies
McMaster University, Hamilton, Ontario

SUMMARY

Development or selection of constitutive relationships for safety analysis or design codes is one of the most important work activities in this CANDU study. In this Chapter, the principle definitions and the approaches used in thermal single-phase and two-phase flow analysis are introduced.

3.1 Introduction

Heat and mass transfer processes in a thermal fluid have been a topic of discussion and controversy for more than a century. In the past decade, a serious examination has taken place, and some insights are beginning to emerge. Nevertheless, most of heat and mass transfer processes in a two-phase flow system are not yet well understood. This state of affairs reflects the great complexity of two-phase flow mass and heat transfer and is perhaps not too surprising when one remembers that even heat and mass transfer processes in single phase turbulent flows still defy prediction from a fundamental point of view. The research approaches conducted in the past are "the empirical approach" and "the analytical approach" (Hewitt 1981). The empirical approach is pragmatically recognizing the need to produce convenient design relationships, and attempts to fit correlating equations of an arbitrary or semi-arbitrary nature to the available experimental data. The limitations of this approach are often self-evident, since we often use the equations on an interpolative or extrapolative basis to predict other cases. However, it forms the basis for the vast majority of design calculations done at the present time. The analytical approach is usually adopted to establish principles first and to derive the governing relationships for two-phase flows. Although the method is mathematically satisfying it does not necessarily lead to a clear physical insight into the problems. Hewitt (1981) suggested that "the phenomological approach" must be used instead of the previous two methods. This approach is invoked to gain physical insight into the phenomena occurring through experiments, and to construct both physical and mathematical models based on this. In this Chapter, an introduction to the phenomenological approach is presented to discuss single- and two-phase flow heat and mass transfer, and to attempt to clarify difficulties in two-phase systems.

3.2 The Phenomenological Approach for Single-Phase Flow

In this approach, the following stages are commonly used:

(1) Identification of the type of flow, and heat or mass transfer or transport processes.

(2) Observation of the detailed phenomena and recording of appropriate measurements such as temperature, pressure, velocity, etc.

(3) Construction of physical models with theoretical links to describe the local phenomena.

(4) Use of the local phenomena for prediction and design.

3.2.1 Identification of the Type of Flow

The type of flow can be categorized as follows:

(1) Newtonian or non-Newtonian flow: interaction between fluid flow and object surface obeys Newton's frictional force law, (Newtonian fluid),

$$\tau = \mu \, du/dy$$

where τ is the shear stress, μ is the viscosity, u is the velocity and y is the direction perpendicular to the object surface. In thermalhydraulics loops, the existence of a fraction of corrosion products in the liquid often changes the liquid behaviour to non-Newtonian type.

(2) Laminar and turbulent flows: motion with irregular velocity fluctuations, we called "turbulent flow". The transition between laminar turbulent flow depends on the geometry of the flow channel, generally around the Reynolds number $Re \gtrsim 10^3$. This Reynolds number is the nondimensional quantity which indicates the relative importance of flow regimes or the viscous nature of the fluid, $U_o L/\nu$, where L is the characteristic length, ν is the kinematic viscosity, and U_o is the average velocity.

(3) Compressible or incompressible flow: a fluid flow subject to a constant density ρ during flow we call "incompressible flow". The transitions between incompressible and compressible flow depends on local fluid velocity, and is generally around the Mach number $M \gtrsim 0.2$. Here the Mach number equals the local fluid velocity/local sound velocity.

3.2.2 Identification of the Type of Heat and Mass Transfer

The type of heat transfer or transmission can be categorized as follows:

(1) Thermal conduction: interchange of thermal energy between molecules.

(2) Thermal radiation: emission of thermal energy in the form of electromagnetic waves.

(3) Thermal convection

(i) Forced convection: transport of hot gas by an external force with and without phase changes

(ii) Natural convection: hot gas moving due to its own thermal buoyant forces, with and without phase changes.

The type of mass transfer or transport can be categorized as follows:

(1) Mass transfer with and without heat transfer or phase change.

(2) Diffusive mass transfer (without convectional effects).

(3) Gravitational driven mass transfer: gravitational factor $Re_g = U_g L/D$ give us the relative importance of gravitational motion and diffusion of mass, where U_g is the terminal settling velocity of particles or bubbles, D_g is the particle or bubble diffusion coefficient.

(4) Convective mass transfer and transport processes; small or low density corrosion particles or bubbles do not affect buffer fluid flow unless the two-phase interaction factor $\Sigma_\phi > 1$, where $\Sigma_\phi = K_\phi L \rho_1/\rho_2 U_s$, K_ϕ is the interfacial drag, U_s is some convenient reference velocity, ρ_1/ρ_2 is the density ratio between the transported and buffer phases.

3.2.3 Heat and Mass Transfer in a Single Phase Flow

The equations for conservation of mass, momentum and energy for an incompressible fluid are respectively as follows:

$$\frac{\partial \rho}{\partial t} + \nabla\cdot(\rho \underline{U}) = 0$$

$$\rho \frac{d\underline{U}}{dt} + \rho(\underline{U} \cdot \nabla)\underline{U} = -\rho \underline{g} \beta (T - T_s) - \nabla P + \nabla\cdot[(\mu + \underline{\varepsilon}) \nabla \underline{U}] \qquad (3.1)$$

$$\frac{\partial T}{\partial t} + \underline{U}\cdot\nabla T = \nabla \cdot (\frac{k}{\rho C_p} \nabla T) + \Phi(U)$$

where T is the temperature, $\Phi(U)$ is the viscous dissipation, β is the coefficient of thermal expansion of the fluid, C_p is the specific heat, k is the thermal conductivity, p is the pressure, ε is the eddy viscosity, and T_s is the reference temperature which is case dependent. If viscous dissipation can be neglected, usually in most cases, the energy equation can be solved without coupling to the mass and momentum conservation equations for $Ra \ll 1$, where Ra is the Rayleigh number ($= g\beta \Delta T_s L^3/\nu\alpha$) and α is the thermal diffusivity. From the nondimensional analysis at constant property conditions (Appendix I) the energy equation becomes the commonly used forced convection heat transport

equation as follows:

$$RePr\ \underline{u}\cdot\tilde{\nabla}\theta - \tilde{\nabla}^2\theta = 0 \qquad (3.2)$$

where Pr is the Prandtl number (= ν/α), θ is the nondimensional temperature, $\tilde{\nabla} = L\nabla$, and u is the nondimensional velocity (U/U_s). Therefore, the heat transfer coefficient, h, depends on the Reynolds and Prandtl numbers, and the formula to calculate the nondimensional heat transfer rate, called the "Nusselt number", is

$$Nu = \left(u_r\theta - \frac{\partial\theta}{\partial r}\right)_{\text{at surface}} \qquad (3.3)$$

where r is the nondimensional directions perpendicular to the surface of objects, and Nu = h L/k. Typical Nusselt numbers obtained from experiment are shown in Appendix II. The results shows significant influences due to the type of flow, as one can observe in Appendix II.

Typical experimental and numerical results obtained in natural convection heat transfer are also shown in Appendix II for various conditions. In this case, the governing equations must be solved in their coupled forms.

The equations of mass transport can be obtained through the multi-phase mass and momentum equations with $\Sigma_\phi << 1$. The nondimensional mass transport equation becomes

$$ReSc\ \underset{\sim}{u}\cdot\tilde{\nabla}\, n - \tilde{\nabla}^2 n = 0 \qquad (3.4)$$

where Sc is the Schmidt number (= ν/D), and n is the nondimensional particle density and D is the diffusion coefficient. From mathematical analogies with the heat transport equation, the experimental and numerical results shown in Appendix II are often used in the mass transfer problems, where the Sherwood number = $Lb/D = (u_r\, n - \partial n/\partial r)$ at the surface and b is the rate of mass transfer.

3.3 The Phenomenological Approach for Two-Phase Flow

In this approach, the following stages are commonly used (Hewitt 1981):

(1) Identification of the flow patterns (or flow regimes).

(2) Observation of the detailed phenomena and the performance of appropriate measurements such as temperatures, pressures, void fractions, quality, flow rates or velocities etc.

(3) Construction of physical models with theoretical links to describe the local phenomena.

(4) Integration of the local models to achieve a complete system description.

(5) Use of the integrated model for prediction and design.

3.3.1 Flow Regime Maps

In gas-liquid two-phase flow in pipes or containers, a number of flow patterns, normally called regimes, are found to exist. This results from the particular manner in which the gas-liquid flow is distributed in the pipe. Even though many authors define flow regimes somewhat differently, most agree with the classification shown in Figure 1:

(1) Stratified smooth flow: this regime often occurs in near horizontal pipes with the liquid at the bottom of the pipe and the gas flow along the top. The surface of the liquid is smooth.

(2) Stratified wavy flow: this flow regime is similar to stratified smooth flow, except that the gas-liquid interface is wavy instead of smooth.

(3) Bubbly flow: this flow regime consists of small, nearly spherical bubbles (gas phase) inside the liquid flow.

(4) Elongated bubble (or plug) and slug flow (intermittent flow, Taitel and Dukler 1976). These flow regimes are characterized by liquid bridging the gap between the gas-fluid interface and the top of the pipe. The difference between slug and plug flow depends on the degree of agitation of the bridge. Plug flow is considered to be the limiting case of slug flow where no entrained bubbles exit in the fluid slug.

(5) Churn flow: this flow regime is similar to that of slug flow except that the gas-liquid interface is wavy and often changing in short times.

(6) Annular flow: this regime occurs when the walls are wetted by a thin film of fluid while gas at high velocity flows through the center of the pipe. Fluid droplets are usually entrained in this gas phase. When the upper walls are intermittently wetted by large aerated waves sweeping through the pipe, it is not included with slug flow, which requires a complete fluid bridge, nor annular flow which requires a stable film. Again, following Barnea et al. (1980), this has been designated as wavy annular flow.

(7) Mist and droplet flow: the gas completely fills the pipe while small liquid drops or mists are distributed through the body of the pipe. The difference between mist and droplet flow depends on the particle size of the liquid phase. Usually if the effect of gravitational motion on the particles is much smaller than diffusion, we call it a "mist".

Identification of flow regimes is not easy in the case of metallic pipes and containers. Detailed methods are discussed in Chapter 17. Some typical flow regime maps based on superficial velocities of gas and liquid phases at the fully developed condition in vertical, horizontal and inclined pipes are shown in Figures 2, 3 and 4, respectively for an air-water two-phase flow at room temperature (Taitel and Dukler, 1976,

Fig. 1: Flow patterns; (a) horizontal flow; (b) vertical flow.

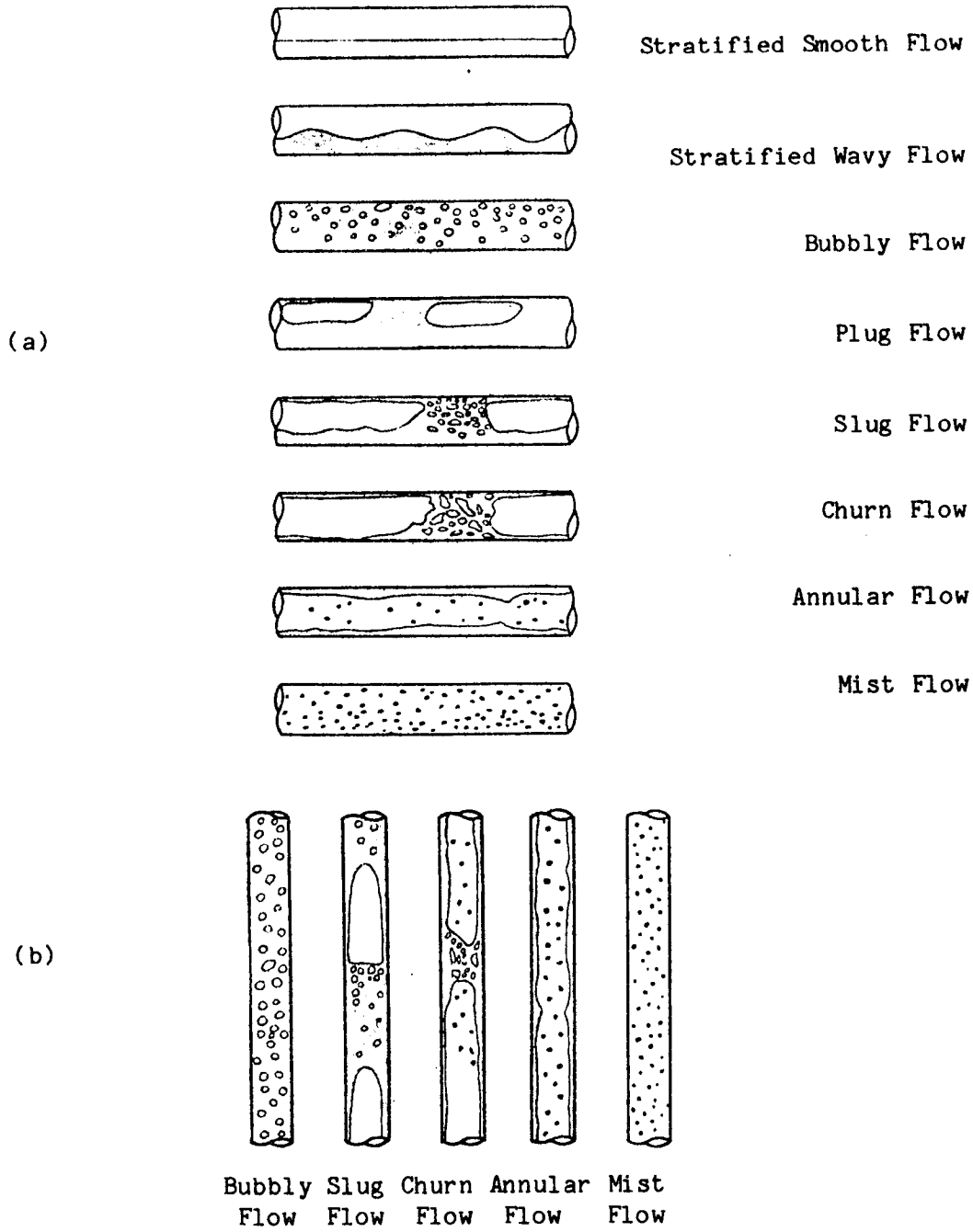

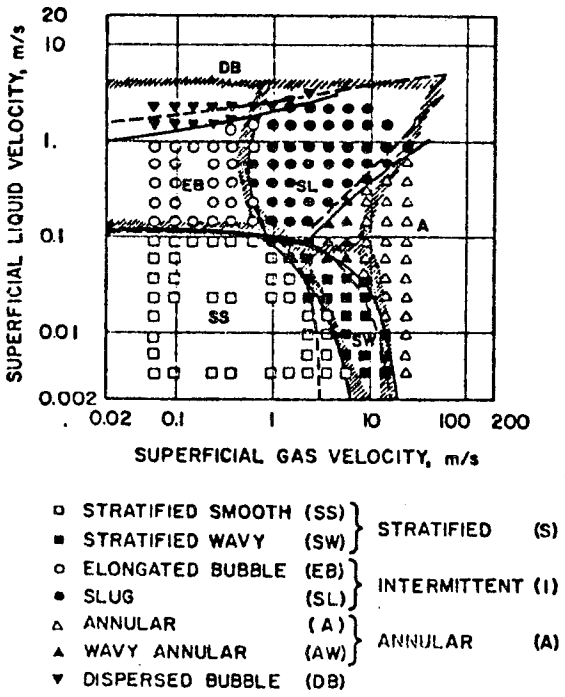

Comparison of data for 2.5 cm horizontal tube with Mandhane *et al.* (1974) Map and Taitel-Dukler (1976) theory. //// Mandhane; — Experiment; -- Theory.

Fig. 2: Flow maps for horizontal tubes. (After [1])

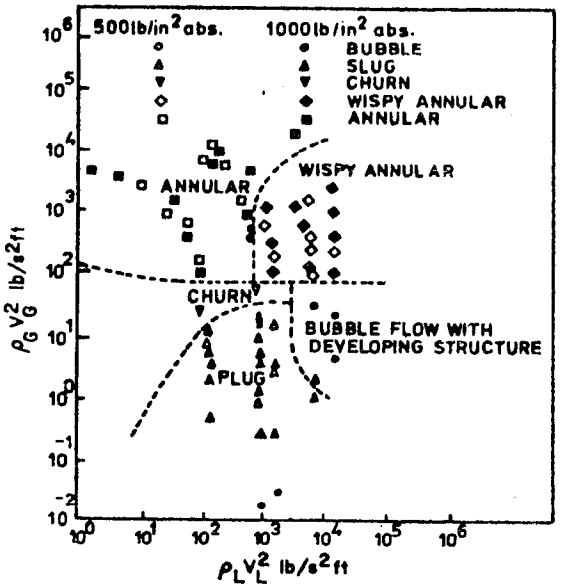

Fig. 3: Flow pattern for vertical tubes (after [10]).

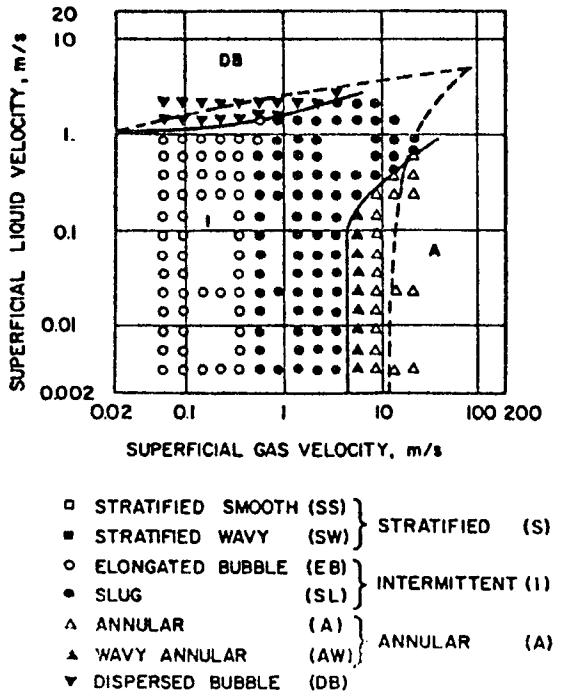

Experimental vs theory. 10° upward inclination of a 2.5 cm pipe. —, experiment; ----, theory.

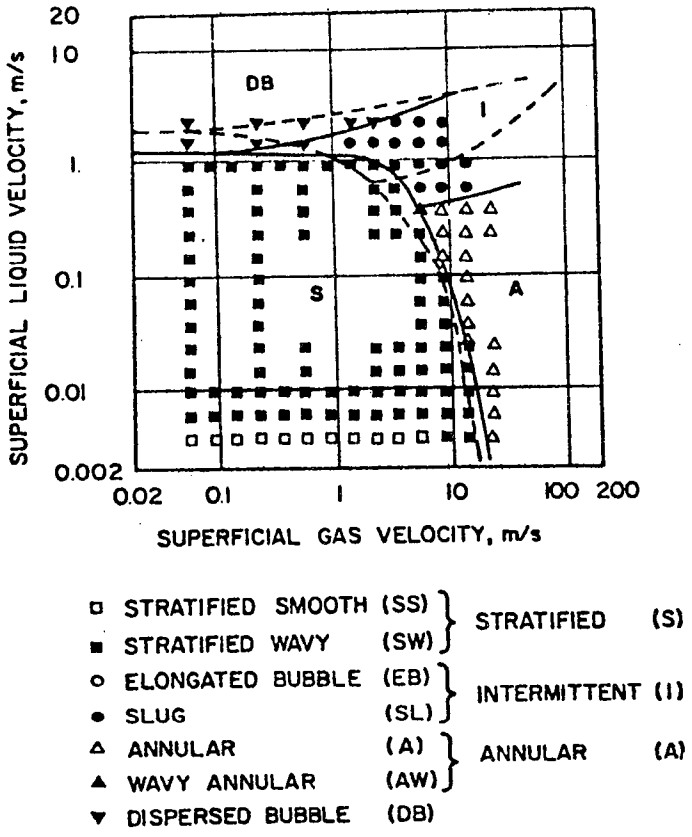

. Experimental vs theory. 10° downward inclination of a 2.5 cm pipe. —, experiment; ——, theory.

Fig. 4: Inclined angle effect on flow pattern maps (after [1]).

Barnea et al. 1980). The descriptions of the transition mechanisms between these flow regimes can be obtained from various references such as Taitel and Dukler (1976).

3.3.2 Flow Quality and Void Fraction

If the mass rates of flow [Kg/s] of the gas and liquid phases are written as $\dot{M}_g$ and $\dot{M}_\ell$, respectively, the "flow quality" x can be defined as

$$x = \dot{M}_g / (\dot{M}_g + \dot{M}_\ell) \tag{3.5}$$

and the total, gas and liquid mass fluxes per unit cross-sectional area, $\dot{m}_t$, $\dot{m}_g$ and $\dot{m}_\ell$, respectively, are given by:

$$\dot{m}_t = (\dot{M}_g + \dot{M}_\ell)/A$$

$$\dot{m}_g = \dot{M}_g/A = \dot{m}_t\, x$$

$$\dot{m}_\ell = \dot{M}_\ell/A = \dot{m}_t\, (1 - x)$$

The value of the flow quality is not usually known locally along a given pipe so is often calculated from the two-phase flow enthalpy h_ϕ. Here the two-phase enthalpy is calculated from the sum of the inlet enthalpy and the heat added up to the location at which flow quality is to be calculated per unit mass of material. Therefore, if h_ℓ and h_g are the liquid and gas phases (saturation enthalpies) respectively, we obtain

$$x = \frac{h_\phi - h_\ell}{h_g - h_\ell}$$

The fraction of pipe occupied by the gas phase is called the "void fraction", ε_g, and the fraction of volume occupied by the liquid is called "hold-up", ε_ℓ, i.e. $\varepsilon_\ell = 1 - \varepsilon_g$.

3.4 Condensing Two-Phase Flow

3.4.1 Type of Condensation

A detailed treatment of condensation and the associated phenomena is not within the scope of this Chapter. It will suffice to highlight a few salient features. Condensation systems may be classified as follows:

1) Indirect contact condensation:

The coolant is separated from the condensing stream by a surface such as a shell- and tube-condenser. Such condensation can take place in the "film-wise" or "drop-wise" modes as shown in Figure 5. In this type of condensation, surface conditions are very important as well as surface materials.

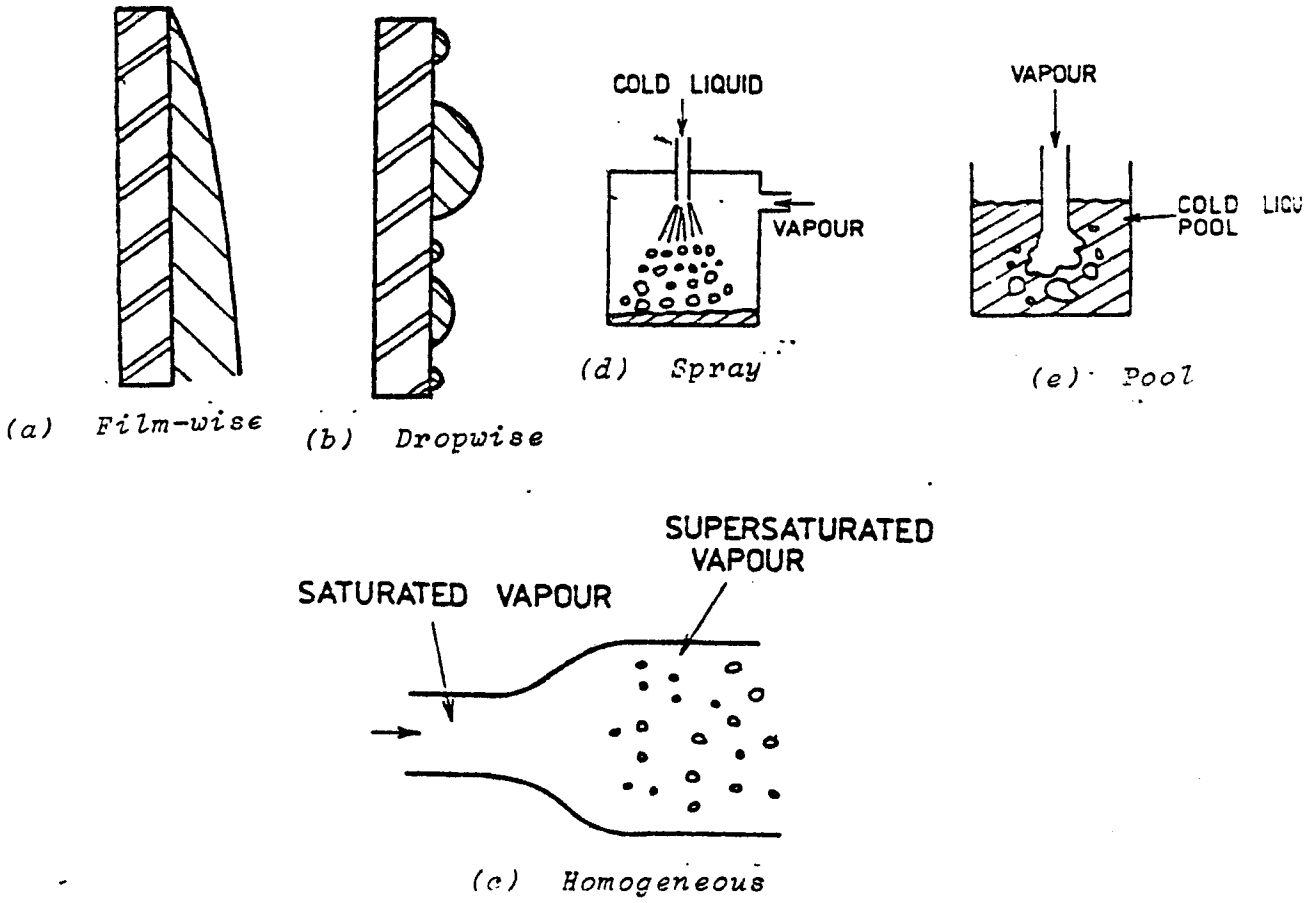

Fig. 5: Modes of condensation.

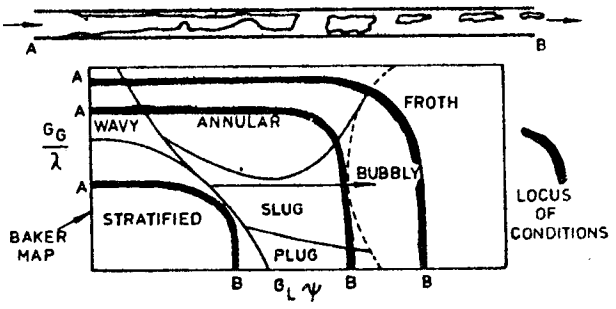

Fig. 6: Flow regimes in condensation in a horizontal tube and their relationship to the Baker (1954) flow pattern map (after [9]).

(2) Homogeneous condensation:

The vapour phase is subcooled and liquid nuclei are formed within the bulk vapour. This type of condensation is not common except during vapour expansion through nozzles as shown in Figure 5.

(3) Direct contact condensation:

The vapour is condensed by direct contact with externally injected cold liquid or recycled condensate. In this type of condensation, the shapes of cold liquid become very important. A typical example of direct contact condensation is shown in Figure 5.

In reactor thermalhydraulics, the following phenomena are typical and important in condensing two-phase flow:

(1) Reflux condensation and thermosyphoning in small break LOCA conditions.

(2) Direct contact condensation in ECC processes.

(3) Homogeneous condensation during blowdowns or small breaks to the atmosphere.

(4) Direct contact condensation during emergency spray cooling conditions.

(5) Direct contact condensation during blow down or small breaks to the secondary side loops, moderator loop, or liquid containers.

(6) Direct contact condensation convective boiling conditions.

3.4.2 Flow Regimes Observed in Condensing Two-Phase Flow

The flow regimes observed in pipes for various inclined angles are shown in Figures 6 and 7. In a vertical pipe with upward vapour flow, flow regimes observed as a function of increasing inlet vapour flow rate are (1) smooth falling film flow (annular); (2) wavy falling film flow; (3) intermittent churn flow; (4) oscillating single phase region on top of counter current churn flow; (5) climbing film flow (annular) (Chang and Girard 1982). These flow regimes are significantly influenced by both secondary side and two-phase interfacial heat removal capabilities. In a horizontal pipe, flow regimes observed as a function of increasing vapour flow rate are very similar to those observed in vertical pipes as follows: (1) smooth stratified flow; (2) wavy stratified flow; (3) intermittent churn flow; (4) intermittent churn flow led by single phase flow (Hewitt 1978). Here we must note that flow reversal is not only observed in vertical pipes but also in horizontal pipes (Wedekind et al. 1972) as well.

The flow regimes observed during water injections to hot or subcooled pipes or the subchannel of tube bundles are shown in Figure 8

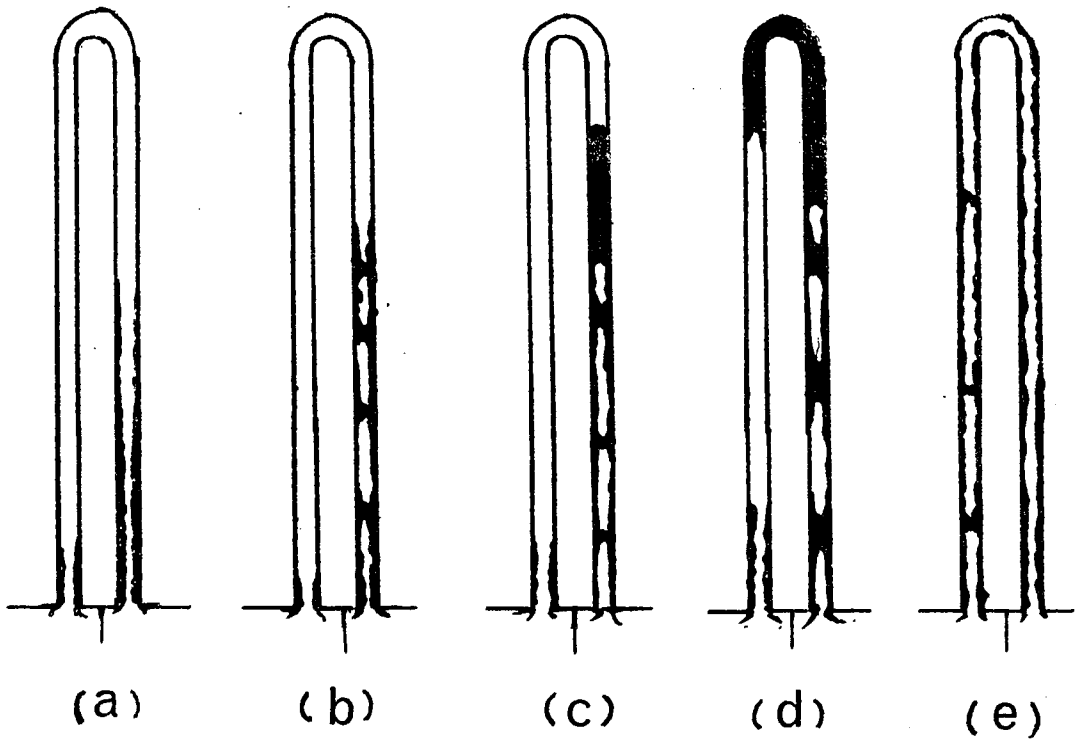

Fig. 7: The sequence of events in U-tube sections leading to two-phase natural circulation (after [11]).

a) falling film flow;
b) churn flow;
c) churn flow with water column;
d) carried over;
e) climbing film flow - two phase natural circulation

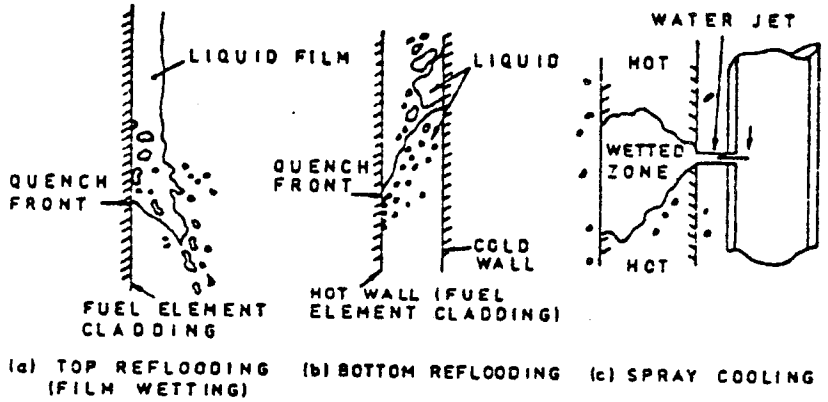

Fig. 8: Types of reflooding for rewetting hot surfaces and condensation of steam.

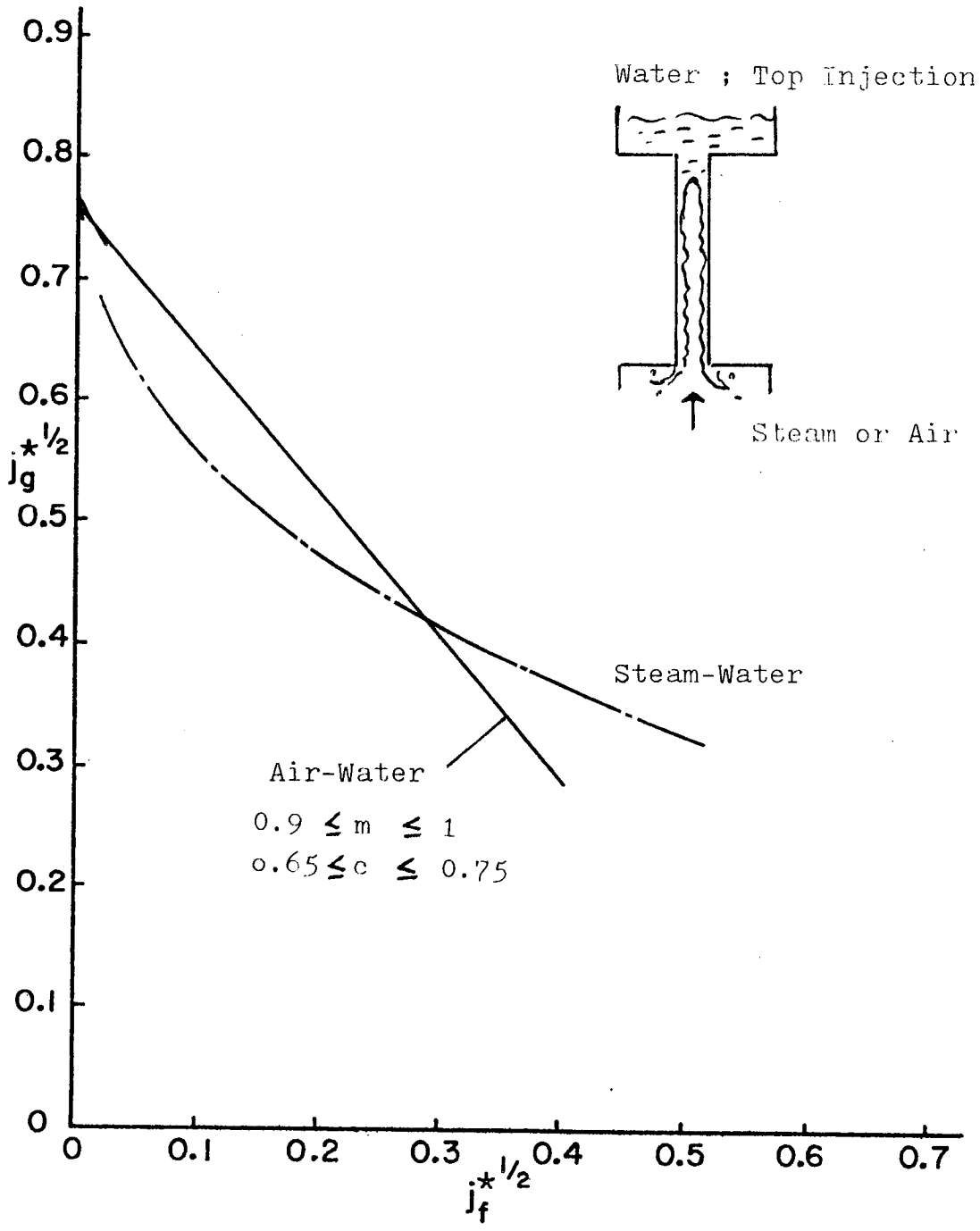

Fig. 9: Top flooding phenomenon, correlations and operating conditions.

for the horizontal and vertical cases. In the vertical condition, a liquid phase supported by a vapour phase is known as the flooding phenomenon. In this case, the coefficient, m, of the general formula for flooding (Wallis correlation)

$$(j_g^{*1/2}) + m\,(j_f^{*1/2}) = C$$

becomes negative in some conditions (Figure 9), since j_g^* is reduced by condensation, i.e. increasing j_g^* (Tien 1977, Wallis et al. 1980), where these dimensionless volumetric fluxes of gas and liquid are defined by

$$j_g^* = \left[\frac{\rho_g\, j_g^{*\frac{1}{2}}}{gL\,(\rho_f-\rho_g)}\right] \quad ; \quad j_f^* = \left[\frac{\rho_f\, j_f^{*\frac{1}{2}}}{gL\,(\rho_f-\rho_g)}\right]$$

where ρ is the density, L is a characteristic length, g is the gravitational acceleration and subscripts f and g refer to liquid and gas, respectively. Here we must note that a rapid direct condensation will generate "condensation shock waves" to form complex condensation and heat transport environment in tubes and containers.

3.4.3 Heat Transfer Rates and Pressure Drops

The theories and experimental correlations on heat transfer rates and pressure drops have been studied by various authors and recently reviewed by Collier (1981). Typical important correlations are summarized in Appendix III. However, the results show considerable discrepancies in the predictions for many processes. These discrepancies influence the determination or prediction of flooding velocity (Deakin 1977), pressure drops (Hewitt 1981) etc. The main problems are due to the influence of various parameters on condensation phenomena; these parameters are summarized as follows:

1. Liquid and gas phase flow rates and local velocity profiles.

2. Two-phase interfacial geometry, area and void fractions.

3. Inclined angles.

4. Liquid and gas properties such as viscosities, thermal expansion coefficients etc., and their temperature and pressure dependencies.

5. The presence of noncondensable gas which reduces heat transport.

6. The effect of non-isothermal wall temperatures.

7. The effect of external forces such as electric and magnetic fields etc.

REFERENCES

1. Barnea, D., O. Shoham, Y. Taitel and A.G. Dukler (1980), Int. J. Multiphase Flow 6, 217-225.

2. Baker, O. (1954), Oil Gas J. 53, 185.

3. Boyko, L.D. and G.N. Kruzhilin (1967), Int. J. Heat & Mass Trans. 10, 361-373.

4. Chang, J.S. and R. Girard (1982), "Advancement in Heat Exchanger", G.F. Hewitt, Ed., Hemisphere Pub., New York.

5. Deakin, A.W. (1977), Harwell U.K., Report No. AERE-M2923.

6. Griffith, P. (1981), "Handbook of Multiphase Systems", Ch. 5, Gittetsroni Ed., Hemisphere Press.

7. Groeneveld, D.C. (1973), AECL Report No. 4450.

8. Hewitt, G.F. (1981), ASME/AICh.E. 20th Heat Transfer Conference, D.Q. Kemn Lecture.

9. Hewitt, G.F. (1978), "Two-phase Flow & Heat Transfer with Application to Nuclear Reactor Design Problem", J.J. Giboux, Ed. Hemisphere Press.

10. Hewitt, G.F. and Roberts, "Handbook of Multiphase Systems", Ch. 5, Gittetsroni Ed., Hemisphere Press.

11. Krishnan, V.S., J.S. Chang and S. Banerjee (1982), Proc. 3rd Canadian Nuclear Soc. Conf., R.C. Oberth Ed., p. A1-6.

12. Mandhane, J.M., G.A. Gregory and K. Aziz (1974), Int. J. Multiphase Flow, 1, 537-553.

13. Sleicher, C.A. and M.W. Rouse (1975), Int. J. Heat & Mass Trans., 18, 677-683.

14. Traviss, D.P., A.B. Baron and W.M. Rohsenow (1971), MIT Report DSR-70591-74.

15. Taitel, Y. and A.E. Dukler (1976), AIChE J., 22, 47-55.

16. Tien, C.L. (1977), Lett. Heat & Mass. Trans. 4, 231-238.

17. Wedekind, G.L., B.L. Bhatt and B.T. Beck (1978), Int. J. Multiphase Flow, 4, 97-114.

18. Wallis, G.B., P.C. deSieyes, R.J. Rosselli and J. LaCombe (1980), EPRI Report NP-1336.

APPENDIX I

By introducing the following nondimensional variables:

$$\underline{u} = U/U_s,\ p = P/\rho_s U_s^2,\ \tau = tU_s/L,\ \tilde{\nabla} = L\nabla,\ Pr = \nu/\alpha,\ Ra = g\beta T_s L^3/\nu\alpha,\ \theta = T/T_s,\ r = R/L,\ R_e = UL/\nu,\ \gamma = \rho/\rho_s,\ \eta = U_s L/\alpha,$$

$$\varepsilon' = \varepsilon/\nu,\ f(\theta) = k(T)\,\rho_s/k(T_s)\rho \qquad (I\text{-}1)$$

we obtain the nondimensional conservation equations from equation (3.1) as follows

$$\frac{\partial \gamma}{\partial \tau} + \tilde{\nabla} \cdot (\gamma \underline{u}) = 0 \qquad (I\text{-}2)$$

$$\frac{\partial(\gamma \underline{u})}{\partial \tau} + (\gamma \underline{u} \cdot \tilde{\nabla})\,\underline{u} = -\,RaPr\,\eta\,(\theta-1) - \tilde{\nabla}p + \tilde{\nabla} \cdot \left(\frac{1+\varepsilon'}{Re}\right) \tilde{\nabla}\underline{u}] \qquad (I\text{-}3)$$

$$\frac{\partial \theta}{\partial \tau} + RePr\ \underline{u} \cdot \tilde{\nabla}\theta = \nabla \cdot (f(\theta)\ \tilde{\nabla}\theta) \qquad (I\text{-}4)$$

where subscript s refers to the reference value which is case dependent.

APPENDIX II

HEAT TRANSFER CORRELATIONS FOR SINGLE PHASE FLOW INSIDE PIPES

Commonly used heat transfer correlations for single phase flow are listed as follows:

(1) Force convection - laminar flow in a pipe (Sieder & Tates' equation 1936)

$$Nu = 1.86\ (Re_f\ Pr_f\ \frac{D}{L})^{1/3}\ (\frac{\mu_f}{\mu_w})^{0.14} \qquad (II\text{-}1)$$

for Re Pr D/L > 12, where D is the tube diameter, L is the tube length, μ is the viscosity.

(ii) Mixed Convection - laminar flow in a pipe (Eubank & Proctor's equation for horizontal pipes).

$$Nu = 1.75\ [\ Re_w\ Pr_w\ \frac{D}{L} + 0.04\ (Gr_w\ Pr_w\ \frac{D}{L})^{0.75}]^{1/3}\ (\frac{\mu_f}{\mu_w})^{0.14} \qquad (II\text{-}2)$$

(Martinelli's equation for vertical pipes)

$$Nu = 1.75\, F_1 \left[Re_w\, Pr_w \frac{D}{L} + 0.0722 \left\{ Gr_w\, Pr_w \frac{D}{L} \right\}^{0.84} F_2 \right]^{1/3} \qquad \text{(II-3)}$$

where F_1 and F_2 are defined in Figure II-1.

(iii) Forced convection - turbulent flow in pipes (Sleicher and Rouse's equations, 1975).

$$Nu = 5 + 0.015\, Re_f^a\, Pr_w^b$$

$$a = 0.80 - 0.24/(4 + Pr_w) \qquad \text{(II-4)}$$

$$b = 1/3 + 0.5 \exp(-0.6\, Pr_w)$$

(for $0.1 < Pr < 10^5$ and $10^4 < Re < 10^6$) where subscripts f and w refer to fluid and wall temperatures, respectively.

(iv) Forced convection - CANDU bundle geometry. In tightly packed bundle geometries the temperature will not be constant around the circumference of the fuel rods due to the poor heat transfer in the gap between two rods. Two approaches may be used:

A. To calculate the temperature of that portion of a rod facing a subchannel, use subchannel code (see Chapter 8) to predict subchannel mass flow and coolant temperature and equations (II1-II4) to predict the heat transfer coefficient (based on equivalent diameter for the subchannel).

B. The procedure discussed by Groeneveld (1973) should be used for predicting the rod surface temperature in the gap between two rods. In this reference a survey has been made of all single phase bundle heat transfer studies in which circumferential temperature distributions were measured.

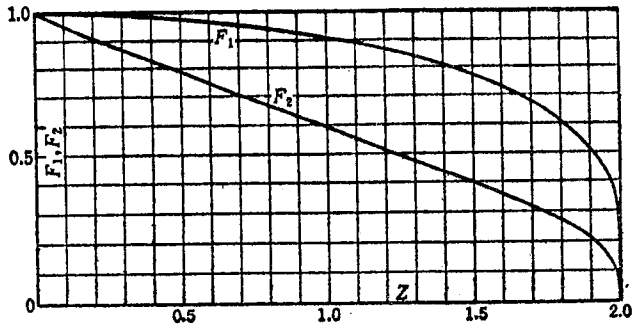

Fig. II-1 F_1 and F_2 for equation (II-3).

APPENDIX III

HEAT TRANSFER RATE AND PRESSURE DROP CORRELATIONS INSIDE PIPES UNDER CONDENSING TWO-PHASE FLOW

Heat transfer rates and pressure drops inside pipes under condensing two-phase flow are not well understood at the present stage. However, the following equations are commonly used in most condenser design.

(i) Heat transfer rate.

(a) Boybo & Kruzhilin's equation (1967) for annular flow

$$\frac{\bar{\alpha} D}{\lambda_\ell} = 0.024 \left(\frac{\dot{m} D}{\mu_\ell}\right)^{0.8} \left(\frac{c_\ell \mu_\ell}{\lambda_\ell}\right)^{0.43} \frac{1 + \sqrt{\rho_\ell / \rho_g}}{2} \qquad \text{(III-1)}$$

(b) Traviss et al.'s correlation (1971) is shown in Figure III-1. The symbols in coordinates are defined as follows

$$Nu = \frac{\alpha(z)\, D}{\lambda_\ell}$$

$$Pr_\ell = \frac{c_\ell \mu_\ell}{\lambda_\ell} \qquad \text{(III-2)}$$

$$Re_\ell = \frac{\dot{m}_\ell D}{\mu_\ell} = \frac{(1 - x)\, \dot{m} D}{\mu_\ell}$$

$$x_{tt} = \left(\frac{\mu_g}{\mu_\ell}\right)^{0.1} \left(\frac{1-x}{x}\right)^{0.9} \left(\frac{\rho_g}{\rho_\ell}\right)^{0.5}$$

where x is the quality, $\bar{\alpha}$ and $\alpha(z)$ are the averaged and local heat transfer coefficients, respectively, D is the tube diameter, λ_ℓ is the thermal conductivity of liquid, μ_ℓ is the viscosity of the liquid, $\dot{m}$ is the mass flow rate, c_ℓ is the specific heat of the liquid, ρ_ℓ and ρ_g are the densities of the liquid and vapour, respectively.

(ii) Pressure Drops.

From the mixture model (see Chapters 5-9), the pressure drops in condensing flow are usually calculated as follows (Griffith 1981),

$$\Delta p_{total} = \Delta p_f + \Delta p_g + \Delta p_m \qquad \text{(III-3)}$$

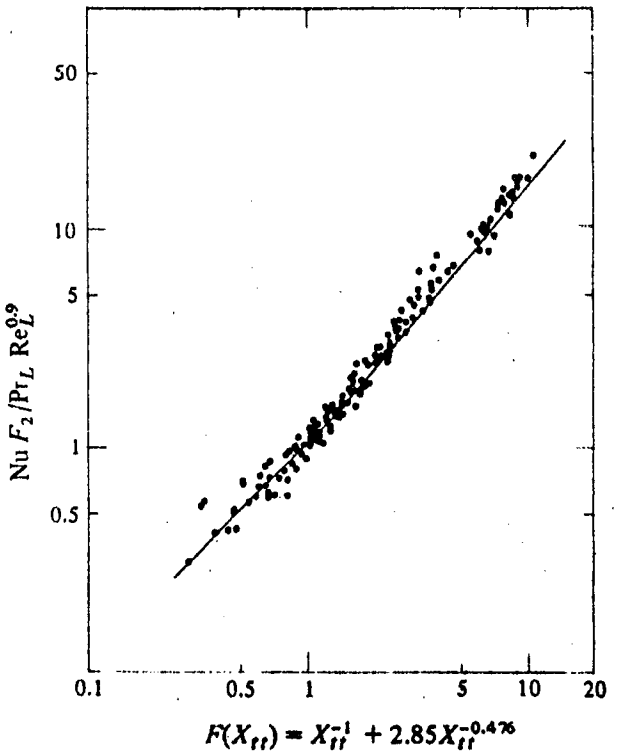

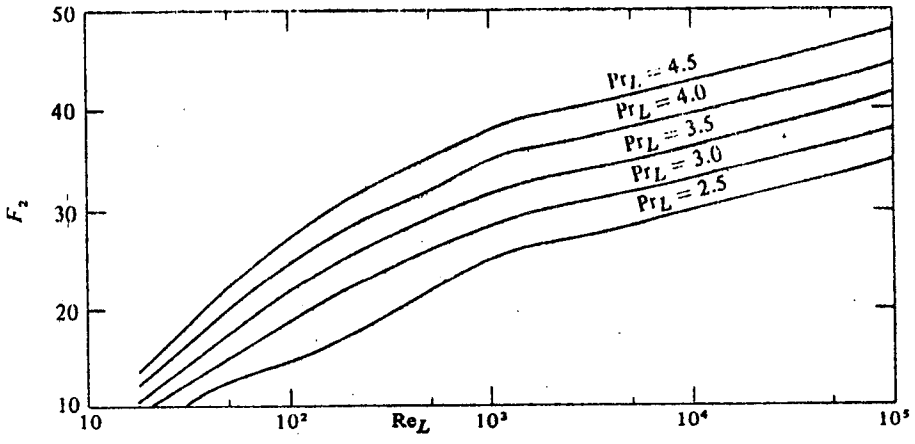

Fig. III-1 Correlation of condensation heat transfer data for tubes of any orientation. This theory has worked well on tubes 1.2 cm in diameter as well as the 1 cm diameter tubes presented here for refrigerants 12 and 22 (Traviss et al. 1971).

$$\Delta p_m = \frac{\dot{m}^2}{g} \left(\frac{1}{\rho_p} - \frac{1}{\rho_g}\right) \qquad \text{(III-4)}$$

$$\Delta p_G = [\rho_\ell (1 - \varepsilon_g) + \varepsilon_g \rho_g] \, g \, L \sin\gamma \qquad \text{(III-5)}$$

where L is the tube length, γ is the inclination angle, Δp_g, Δp_m, Δp_f is the pressure drop by gravity, momentum and friction, respectively (see detail in Chapters 5-9).